Investigation on Forming Limit Properties of Dual Phase Steel

Libo Pan[a], Bernard Rolfe[b], Alireza Asgari[b], Matthias Weiss[b], Zhijian Zhang[a]

[a] *Research and Development Center of Wuhan Iron and Steel (Group) Corp.,430080,Wuhan, China*
[b] *Institute for Frontier Materials, Waurn Ponds Campus, Deakin University, Geelong 3217, Victoria, Australia*

Abstract. The accurate representation of the forming limit properties in the material model is very important for predicting the onset of failure. In this study, the FLCs for two dual phase steels DP780 and DP600 were experimentally obtained. The FLSCs were derived numerically by setting up stretching models in ABAQUS in which experimental FLD data were employed as failure criteria. The results of FLSCs showed in good agreement with that transformed from theoretical calculation. A new type of forming limit diagram based on Polar representation of EPS (Effective Plastic Strain) which proposed by Stoughton and Yoon was conducted to analyse the difference of result caused by FLD and FLSD criteria. The forming processes of a special cup-type part drawing were modelled and simulated by utilizing FLD and FLSD as failure criteria, respectively. According to analysis, the Polar EPS diagram can intuitively describe formability problems in forming processes. To avoid the occurrence of failure, it was found that if strain path for the final stage in Polar EPS diagram can be controlled to locate in some safe zones which can be expressed by function related to some parameters, certain required EPS could be achieved without failure during forming. The results indicated that Polar EPS Diagram seemed to be a good tool to analyse formability in complex strain paths condition and could be used to strengthen formability by designing nonlinear paths.

Keywords: Dual Phase Steel, Forming Limit, Polar EPS Diagram.

INTRODUCTION

Advanced High Strength Steels are being used to reduce weight and increase safety in passenger car bodies. They exhibit good strength and ductility, but their forming properties may be difficult to evaluate. Practical testing of forming applications has been replaced to some extent by numerical simulation to shorten lead times and reduce costs. The accuracy of the material model used in the simulation significantly influences the precision of the prediction. The accurate representation of the forming limit properties in the material model is vital since they define the onset of failure in the simulation

The Forming limit Diagram (FLD) is an effective concept for characterizing the formability of sheet metals [1]. It represents the maximum major and minor strains that are achievable in the forming of a specific sheet metal before the onset of necking and has been used as a failure criterion for the past decades [2]. However, the FLD has several shortcomings, such as being easily influenced by friction and only being suitable for linear strain path forming. If in a sheet forming process the loading path is nonlinear, the FLD does not accurately predict material forming limits and recent studies have focused on the development of strain path independent characterisation methods to estimate material forming limits in sheet forming processes. The Forming Limit Stress Diagram (FLSD) was found to be an ideal method to substitute the strain based FLD as a failure criterion due to its independence to strain paths [3, 4]. In the FLSD the forming limits are plotted on a principal stress field instead of a principal strain field as it is the case for the FLD. In this way the limits are positioned on one curve regardless of their loading path histories giving forming limits that are valid for any nonlinear loading path [5]. Additionally to that Stoughton and Yoon [6] introduced the Polar Effective Plastic Strain (EPS) diagram to intuitively describe formability problems in forming processes. The method has a one-to-one mathematical correspondence with the FLSD and is independent of the stress-strain relation. This approach which was developed based on ideas proposed by Yoshida et al. [7] and Zeng et al[8]indicated that the forming limit for nonlinear deformation can be characterized as function on effective plastic strain and the ratio of the current strain rates.

In this study, the FLDs of two dual phase steels, a DP780 and a DP600 were determined experimentally and FLSD derived from the strain based forming limit results. By employing the FLD and the FLSD respectively as failure criteria the stretch forming process was simulated. The Polar EPS Diagram was conducted to explain the high difference between FLD and FLSD numerical predictions. Strain path can be designed to avoid failure during forming process through analysis in Polar EPS diagram. The results indicate that the Polar EPS Diagram is a useful tool to analyse formability for forming processes including complex strain paths conditions.

The 11th International Conference on Numerical Methods in Industrial Forming Processes
AIP Conf. Proc. 1532, 850-856 (2013); doi: 10.1063/1.4806920

MATERIALS CHARACTERIZATION

The materials used in this study were DP780 with a thickness of 2mm and DP600 with a thickness of 1mm.The tensile tests were performed in an Instron 100KN and samples were prepared in three directions, parallel, diagonal and transversal to rolling direction. Both materials showed a plastic strain ration $r \sim 1$ and very similar stress strain relationships were observed for the three directions tested (**FIGURE 1(a)** and **(b)**) which indicates almost ideal material isotropy.

The FLD tests were conducted in accordance with the ISO 12004-2 standard in an Erichsen sheet metal tester. Chemically etched specimens with various widths were stretch formed over a hemispherical punch and an optical grid analysing system was used to determine the forming limit strains. The FLDs for the two materials are shown in **FIGURE 1(c).**

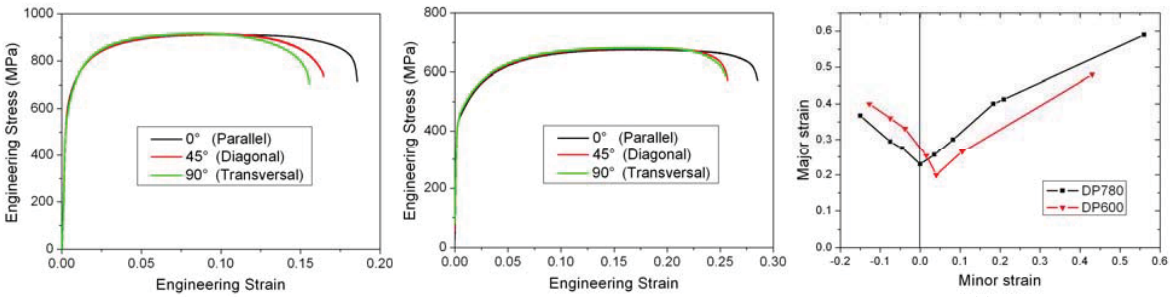

FIGURE 1. Mechanical Property Results for Two Materials
(a) Stress-strain Curves for DP780 (b) Stress-strain Curves for DP600 (c) FLCs for Two Materials

Since there is no reliable way to determine the stresses inside the material during forming it is impossible to generate FLSD from experimental data only. By Stoughton's calculating method [4], FLSDs can be obtained by theoretical calculation. A developed commercial code also allows obtaining the stress state on deformed parts during forming using numerical analysis. A finite element model of the forming limit test was set up in the commercial code Abaqus using shell elements with reduced integration (S4R). Only damage initiation was employed in this study to determine the onset of failure using the forming limit strains determined in the experiments. An isotropic elastic-plastic material model with hardening described by power law was used for both, the DP780 and the DP600. The different stress states in elements where failure took place (as shown in **FIGURE 2**) were extracted as forming limit stress data. FLSDs results for two materials were also theoretically calculated by Stoughton's calculating method [4]. **FIGURE 3** shows the FLSCs for both materials determined by the numerical model and the results indicated good agreement with that from theoretical calculation.

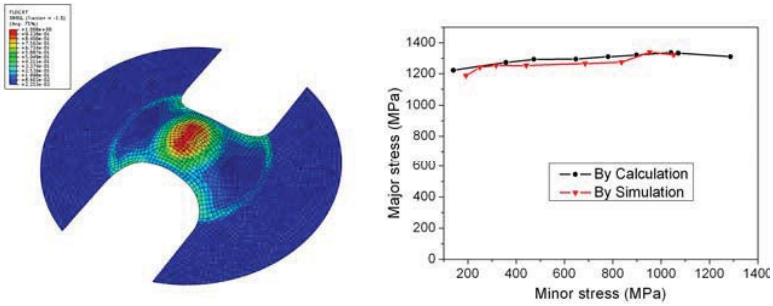

FIGURE 2. Simulation Result when FLDCRT=1

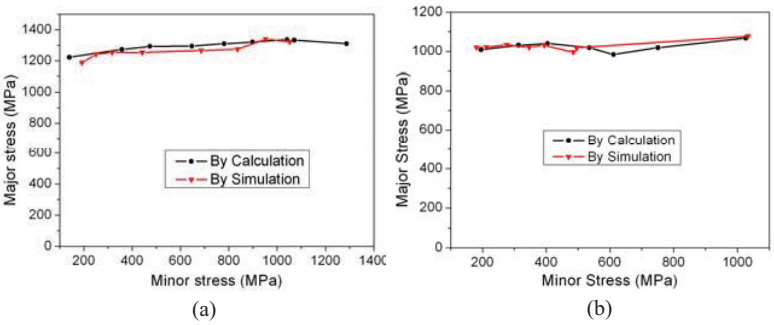

FIGURE 3. FLSD Result (a) DP780 (b) DP600

FORMING SIMULATION

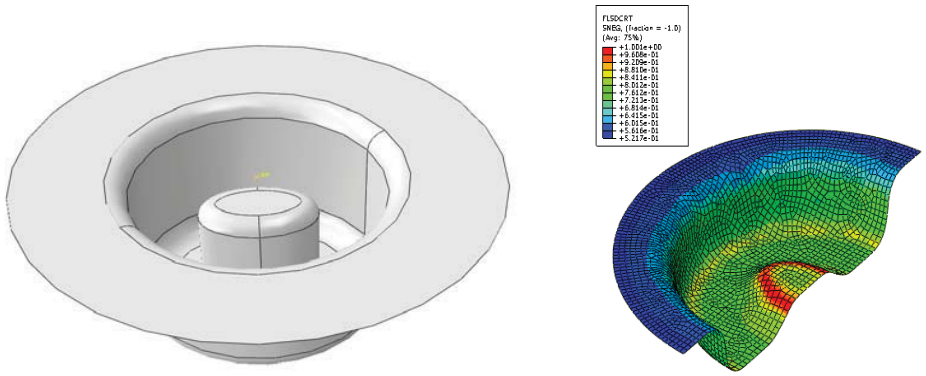

(a) (b)

FIGURE 4. Die Shape and Simulation Result for DP780
(a) Illustration of Die (b) Simulation Result

To verify the new approach of Polar EPS Diagram proposed by Stoughton and Yoon [6], the forming process of a cup-type part which contained two drawing steps was numerically analysed. The die was designed as shown in **FIGURE 4(a).** In this model, a cylindrical cup shape was deep drawn in the first forming step to form an equal-biaxial strain condition. Then in the second forming step, an oval-shaped punch was used in the central area to draw in the opposite direction which was supposed to result in a large change in strain path between two steps. The finite element model was established in Abaqus/Explicit and the same material models used in FLSD simulation above were applied. To find the prediction difference between FLD and FLSD criteria, the FLD and FLSD data for these two materials were employed as damage criteria to predict failure. For all cases, the interfaces between blanks and rigid surfaces were modeled with surface-to-surface contact algorithm. The friction coefficients between blank surfaces and the rigid surfaces of the punch and the die were set to 0.2, and a friction coefficient of 0.3 was used for the contact between the blank surface and the blank holder to apply a specific withdrawing force, the blank holding forces were 50kN for DP780 and 40kN for DP600. Shell elements with reduced integration (S4R) were utilized in the model.

RESULT AND DISCUSS

As shown in **FIGURE 4 (b)**, during forming the area along the corner surrounding flat end was risky for failure. Strain paths in some elements along this area at different punch displacements were analysed. As shown in **FIGURE 5**, strain paths history and stress status of Element 1410, 614, 2017 and 604 were extracted and plotted in FLD and FLSD, respectively. It can be seen that there were changes in the strain paths for these elements during forming and strain history (**FIGURE 5 (c)**) could be divided into several piecewise linear strain paths. In this forming case FLSD predicted failure much earlier than FLD. For instance, element 1410, 614 and 2017 were safe in FLD as shown in **FIGURE 5(c)**, whereas FLSD criterion showed these elements began to fail (**FIGURE 5 (d)**). Strain status for these four elements were analysed in Polar EPS diagram as showed in **FIGURE 6** which indicated similar result to that in FLSD. By Polar EPS diagram, it can be clearly explained how these elements were failed or safe under corresponding strain paths condition and why there were differences between predictions of FLD criterion and FLSD criterion. The key point is the changes in strain path history. The simulation for DP600 also showed similar result to that for DP780. Polar EPS diagram seemed to be an intuitive and effective method to determine failure.

By analysing the Polar EPS diagram, to get a high formability, no matter what type of strain conditions in the previous stages were, the strain status at the final stage of forming should optimally be uni-axial or equal-biaxial strain condition which would make material undertake much large effective plastic strain without exceeding the forming limits, and strains in previous stages mainly contributed to the amount of effective plastic strain. Reversely, if the strain path at final stage was close to plane strain condition, it would be very likely to reach failure. It can be

deduced that different changes for strain paths will result in different prediction between FLD and FLSD criteria. For example, if θ stood for the angle between strain path and major strain axis, the absolute value of θ in the final stage of strain paths for element 614 in **FIGURE 6 (b)** was comparatively small which meant strain status was close to plain strain condition, then, failure predicted by FLSD possibly took place much earlier than that by FLD. On the contrary, during forming if the strain paths in early stages were close to plane strain condition and the strain path in the final stage tended to equal-biaxial strain condition, FLSD would supposedly predict failure later than FLD. According to analysis, the main factors affecting formability during forming were total effective plastic strain and strain status at the final stage of nonlinear strain path.

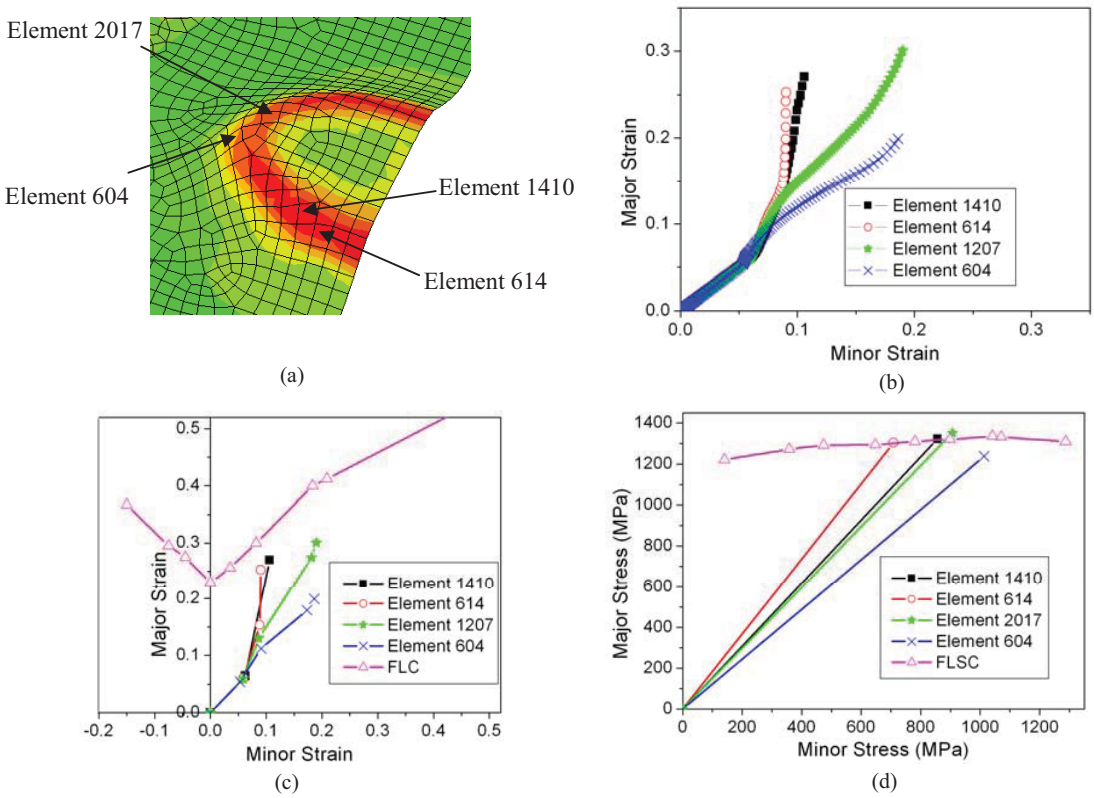

FIGURE 5. Results with Different Forming Limit Diagram
(a) Locations for Selected Elements (b) Strain PathsHistory (c) FLD (d) FLSD

As shown in **FIGURE 7**, given certain effective plastic strain $\bar{\varepsilon}_f$ was required in some area of the part during forming, the circle of $\bar{\varepsilon}_f$ in Polar EPS diagram intersected with forming limit curve at two points *C* and *D*. Line *OA* represented equal-biaxial strain condition with $\varepsilon_2 / \varepsilon_1 = 1$, and Line *OB* stood for uni-axial strain condition with $\varepsilon_2 / \varepsilon_1 = -0.5$. θ_1 and θ_2 were the angles for strain state direction when strain state reached forming limit curve in the right side and left side of diagram, respectively. It was evident that θ_1 should be positive and θ_2 was negative. To keep this area safe with effective plastic strain of $\bar{\varepsilon}_f$ during forming, the angle of strain direction at the final stage θ would have some range or limitations.

To analyse the safe conditions more conveniently, the FLC for the material could be simplified to two lines in left and right sides, the forming limit curve in Polar EPS diagram were composed of two lines correspondingly in two sides, with angle φ_1 and φ_2, respectively, as shown in **FIGURE 7**, the intercept for forming limit curve with y axis was $\bar{\varepsilon}_0$. The functions for two forming limit lines can be expressed as follows:

$$y = \bar{\varepsilon}_0 + x / \tan\varphi_1 \qquad (x > 0, \varphi_1 > 0) \tag{1}$$

$$y = \bar{\varepsilon}_0 + x / \tan\varphi_2 \qquad (x < 0, \varphi_2 < 0) \tag{2}$$

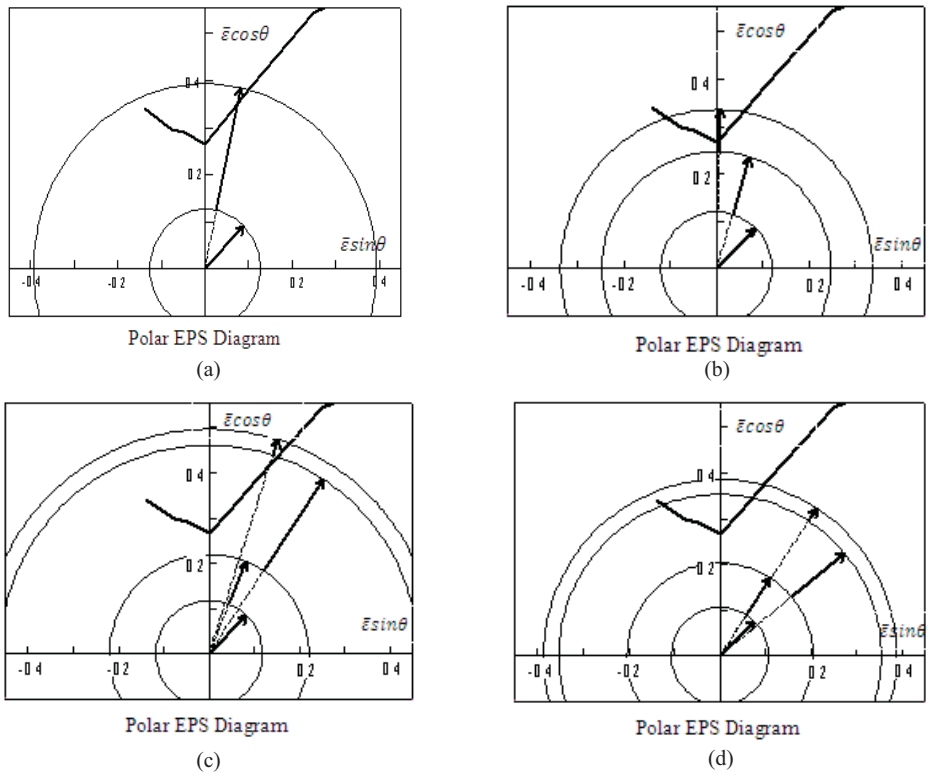

FIGURE 6. Results in Polar EPS Diagrams
(a) Element 1410 (b) Element 614 (c) Element 2017 (d) Element 604

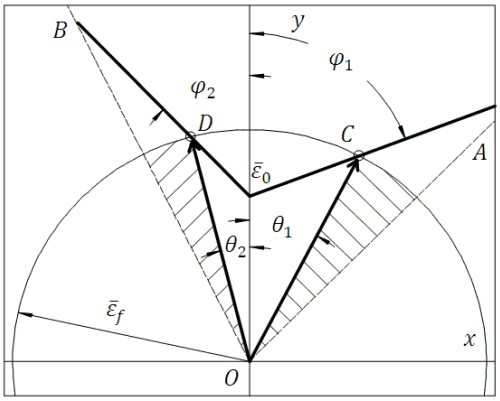

FIGURE 7. Strain Condition Analysis in Polar EPS Diagram

The function for the circle of required effective plastic strain in Polar EPS diagram can be expressed by

$$x^2 + y^2 = \bar{\varepsilon}_f{}^2 \tag{3}$$

If $\bar{\varepsilon}_f < \bar{\varepsilon}_0$, failure would not occur during forming no matter what kind of strain condition it experienced, however, when $\bar{\varepsilon}_f < \bar{\varepsilon}_0$, the intersection point C and D can be worked out according to equations (1), (2) and (3). The coordinate vector in x axis can be obtained, then θ_1 and θ_2 can be expressed by the following equations.

$$\theta_1 = \sin^{-1} \frac{\sqrt{[1+(\tan\varphi_1)^2]\bar{\varepsilon}_f{}^2 - (\bar{\varepsilon}_0 \tan\varphi_1)^2} - \bar{\varepsilon}_0 \tan\varphi_1}{1+(\tan\varphi_1)^2} \tag{4}$$

$$\theta_2 = \sin^{-1} \frac{-\sqrt{[1+(\tan\varphi_2)^2]\bar{\varepsilon}_f{}^2 - (\bar{\varepsilon}_0 \tan\varphi_2)^2} - \bar{\varepsilon}_0 \tan\varphi_2}{1+(\tan\varphi_2)^2} \tag{5}$$

From FIGURE 7, when $\theta_2 \le \theta \le \theta_1$, failure would take place , however, under the condition of $-26.5° < \theta \le \theta_2$ or $\theta_1 \le \theta \le 45°$, as shown in the shadow area with profile lines, safety could be achieved. Then the safe condition about the strain status during forming can be expressed by

$$-26.5° < \theta \le \sin^{-1} \frac{-\sqrt{[1+(\tan\varphi_2)^2]\bar{\varepsilon}_f{}^2 - (\bar{\varepsilon}_0 \tan\varphi_2)^2} - \bar{\varepsilon}_0 \tan\varphi_2}{1+(\tan\varphi_2)^2} \tag{6}$$

Or

$$\sin^{-1} \frac{\sqrt{[1+(\tan\varphi_1)^2]\bar{\varepsilon}_f{}^2 - (\bar{\varepsilon}_0 \tan\varphi_1)^2} - \bar{\varepsilon}_0 \tan\varphi_1}{1+(\tan\varphi_1)^2} \le \theta \le 45° \tag{7}$$

Generally the ideal state for maximum formability is keeping linear strain path in uni-axial or equal-biaxial strain condition which is impossible for the whole stamping part to achieve. Actually in practical stamping, some special means can be used in critical area where failure took place easily to change the strain path into equal-biaxial condition. With the safe condition obtained in expressions (6) and (7), guidance can be given for the strain path status during forming process to achieve safe deformation.

CONCLUSIONS

Forming limit properties are very important in practical forming of AHSS. It is a more reliable way to use FLSD as failure criterion instead of FLD which is not suitable for nonlinear strain path condition.

(1) The new approach Polar EPS diagram deduced from FLSD seemed to be similarly effective as FLSD but more intuitive and specific.

(2) By analysing strain paths condition in this diagram, to keep material safe during forming process, strain status should meet some requirement.

(3)By using Polar EPS diagram to analyse strain status, high performance of formability in practical forming may be achieved through appropriate strain path changing.

ACKNOWLEDGEMENT

The authors would like to thank Professor John Duncan from Auckland University and Professor Peter Hodgson in Deakin University for indications and help in understanding metal forming limit and discussing models and simulation.

REFERENCES

1. G. C. Ramos, M. Stout and R. E. Bolmaro, etc, *Int. J. Solids Struct.,* **47**, pp.2294-2299 (2010)
2. M. Firat, *Mater. Design*,**34**, pp.32-39 (2012)
3. R. Arrieux, C. Bedrin and M. Boivin, Proceedings of the 12th Biennial Congress of the IDDRG, pp.61-71.

4. T. B. Stoughton, *Int. J. Mech. Sci.***42**, pp.1-42 (2000)
5. T. Iguchi, *ISIJ Int.*,**47(3)**, pp. 493-501 (2007)
6. T. B. Stoughton and J. W. Yoon, *Int. J. Solids Struct*., (2012), http://dx.doi.org/10.1016/j.ijsolstr.2012.08.004
7. K. Yoshida, T. Kuwabara and M. Kuroda, *Int.J. of Plasticity*,**23**, pp.361-384 (2007)
8. D. Zeng, L. Chappuis, Z. C. Xia and X. Zhu, SAE 01-1445 (2008)